

Mars 1977

INT. 80/77

A CROSS-POWER SPECTRUM ANALYZER

M. Bitter, Ch. Hollenstein, P.J. Paris and C. Rizzo

Centre de Recherches en Physique des Plasmas

ECOLE POLYTECHNIQUE FEDERALE DE LAUSANNE

## A CROSS-POWER SPECTRUM ANALYZER

M. Bitter, Ch. Hollenstein, P.J. Paris and C. Rizzo

Ecole Polytechnique Fédérale de Lausanne, Switzerland  
Centre de Recherches en Physique des Plasmas

### INTRODUCTION

A measurement of the cross correlation function or the cross-power density spectrum is an important means for the analysis of noise. Different analog and digital devices have been developed /1/. We have built an analog cross-power spectrum analyzer following the design of Harker and Ilić /2/.

This note is to be understood as a manual for the use of this instrument. It contains a short summary of the basic relations of noise analysis and the instrumental specifications. We also report on first experimental applications to magnetized and unmagnetized low density plasmas.

1. BASIC RELATIONS OF NOISE ANALYSIS

---

The turbulent state of a plasma is characterized by the "wave spectral density"  $|\phi_{(\omega, \vec{k})}|^2$  of a fluctuating quantity  $\phi_{(x, t)}$  like electron density or plasma potential. The wave spectral density can be determined from a measurement of the "cross correlation function", which is defined as

$$(1) \quad C(x, \chi, \tau) = \lim_{T \rightarrow \infty} \frac{1}{T} \int_{-T/2}^{T/2} \Phi(x, t) \Phi(x + \chi, t + \tau) dt$$

where the fluctuating quantity  $\phi_{(x, t)}$  may be represented by the electron or ion saturation current derived from Langmuir probes at the positions  $x$  and  $x + \chi$ . Using the Fourier representation  $\phi \sim \int d\omega \int d^3k \phi_{(\omega, \vec{k})} e^{i(\omega t + \vec{k}\vec{x})}$  and the identity  $\delta(\omega + \omega') \sim \lim_{T \rightarrow \infty} \frac{1}{T} \int_{-T/2}^{T/2} e^{i(\omega + \omega')t} dt$ , we obtain

$$(2) \quad C(x, \chi, \tau) = \int d\omega C(x, \chi, \omega) e^{i\omega\tau}$$

where

$$(3) \quad C(x, \chi, \omega) \sim \int d^3k \int d^3k' \Phi(\omega, \vec{k}) \Phi(-\omega, \vec{k}') e^{i(\vec{k} + \vec{k}')x} e^{i\vec{k}'\chi}$$

is the "cross-power density spectrum".

For certain cases the expression for the cross-power density spectrum assumes simpler forms:

(a) The fluctuations are independent of  $\vec{X}$ . Expression (3) can be averaged over  $\vec{X}$ . Using the appropriate definition for  $\delta(\vec{k} + \vec{k}')$  and the identity  $\phi(-\omega, -\vec{k}) = \phi_{(\omega, \vec{k})}^*$ , since  $\phi_{(x, t)}$  is real, we obtain

$$(4) \quad C(\chi, \omega) \sim \int d^3 k |\Phi(\omega, \vec{k})|^2 e^{-i\vec{k}\chi}$$

Thus, the wave spectral density  $|\Phi(\omega, \vec{k})|^2$  is the inverse spatial Fourier transform of  $C(\chi, \omega)$ .  $C(0, \omega)$  is the "frequency power spectrum" of the fluctuations.

(b) Weak turbulence.  $\omega$  and  $\vec{k}$  are connected by a dispersion relation  $\omega = \omega(\vec{k})^*$ . It is not always necessary to perform the inverse spatial Fourier transform of  $C(\chi, \omega)$ , since  $|\Phi(\omega, \vec{k})|^2$  can be obtained from appropriate measurements. As an example we consider a one-dimensional case. The wave spectral density assumes the form /2/:

$$(5) \quad |\Phi(\omega, \vec{k})|^2 = \delta(k_2) \delta(k_3) \left\{ \Phi_{k_1}^2 \delta[\omega - \omega(k_1)] + \Phi_{-k_1}^2 \delta[\omega - \omega(-k_1)] \right\}$$

$$= \frac{\delta(k_2) \delta(k_3)}{v_g} \left\{ \Phi_{k_1}^2 \delta[k_1 - k_1(\omega)] + \Phi_{-k_1}^2 \delta[k_1 + k_1(\omega)] \right\}$$

and we obtain

$$(6) \quad C(\chi, \omega) \sim \frac{1}{v_g} \left\{ \Phi_{k_1}^2 e^{ik_1(\omega)\chi_1} + \Phi_{-k_1}^2 e^{-ik_1(\omega)\chi_1} \right\}$$

or

$$(7) \quad \text{Re } C(\chi, \omega) \sim \frac{1}{v_g} \left\{ \Phi_{k_1}^2 + \Phi_{-k_1}^2 \right\} \cos k_1(\omega)\chi_1$$

$$(8) \quad \text{Im } C(\chi, \omega) \sim \frac{1}{v_g} \left\{ \Phi_{k_1}^2 - \Phi_{-k_1}^2 \right\} \sin k_1(\omega)\chi_1$$

The following results can be obtained from measurements of  $\text{Re } C$  and of  $\text{Im } C$  : Using Langmuir probes, which look simultaneously in both directions, we obtain the frequency power spectrum from a measurement of  $\text{Re } C(0, \omega)$ . For a given  $\chi_1 \neq 0$ ,  $\text{Re } C(\chi_1, \omega)$  and  $\text{Im } C(\chi_1, \omega)$  are oscillating functions of  $\omega$ . The dispersion relation  $\omega(k_1)$  can be derived from the period of these oscillations ( $k_1 = \frac{\omega}{c}$  for a linear

---

\* A well defined dispersion relation does not exist for large amplitude fluctuations (strong turbulence) owing to non-linear effects.

dispersion relation). The amplitude of the oscillating functions  $\text{Re } C(\chi_1, \omega)$  and  $\text{Im } C(\chi_1, \omega)$  is a measure of the frequency power spectrum and of the anisotropy of the wave spectral density, respectively. The ratio of  $\phi_{k_1}^2$  and  $\phi_{-k_1}^2$  can be measured by the use of single face plane Langmuir probes, which are successively turned in both directions.

## II. INSTRUMENTAL SPECIFICATIONS

---

The principle of operation can be understood with the aid of fig. 1a,b. (The detailed circuit is shown in fig. 1c.) The signals, which enter into the channels 1 and 2, are shifted up in frequency, in order to perform the products of the "in phase" signals and of the "90 degree out of phase" signals at a single frequency  $\nu_0$ . The time averages of these products are proportional to  $\text{Re } C(\chi, \omega)$  and  $\text{Im } C(\chi, \omega)$ .

The instrument operates in the range  $0 < \nu < 12\text{MHz}$ , which covers the range of low frequency turbulence (current driven ion acoustic turbulence, ion-beam excited and drift wave instabilities) for many low density plasma experiments. The study of high frequency electron plasma wave noise would require an instrument, which operates in a typical frequency range from . 1 to 3 GHz.

Critical components are the multipliers, the narrow band filters at  $\nu_0 = 6\text{ MHz}$  and the mixers, which determine the transfer function of the two channels. The response of the multipliers (Motorola MC 1496L) is linear for input signals up to 40 mV. The filters are quartz filters of  $\pm 18\text{ KHz}$  bandwidth (60 dB at  $\pm 40\text{ KHz}$ ), since reliable high Q filters could not be realized with RLC circuits for this frequency due to the occurrence of stray capacitances. The frequency response of the filters is shown in Fig. 2.\* We see from fig. 2 that the frequency response of the

---

\*The ondulation has been specified by the manufacturer (Compagnie d'Electronique et de Piézo-Electricité, 101, Rue du Pt.-Roosevelt, 78500 Sartrouville, France) as . 5 dB and 1.3 dB, respectively.

filters is very similar and can be approximated by a constant over the narrow frequency range ( $6 \pm .018$  MHz).

The phase shift introduced by a narrow band filter is  $m\pi$  ( $m = 1, 2, 3, \dots$  see theory of filter response). The difference of the phase shifts introduced by the quartz filters was found to be an odd multiple of  $\pi$ . This was compensated by using the inverted output of the succeeding amplifier in one of the channels.

The function of the mixers needs a detailed consideration. The mixers (HP 10534A) are double balanced with an input isolation of better than -50 dB for frequencies up to 20 MHz. The response is proportional to the amplitude of the modulating signal up to 400 mV, if the mixers are properly switched by the carrier signal. This is achieved by a sine wave signal of 1.5 volt amplitude, which drives the diodes into saturation. Therefore the output signal contains the carrier signal as a square wave. As an example we show in fig. 3 the output signal obtained for a modulating sine wave ( $V_M \sin \omega_M t$ ). This signal can be represented in the form

$$V_{out} \sim V_M \sum_0^{\infty} \frac{1}{2n+1} \sin [(2n+1)\omega_c \pm \omega_M]t$$

Thus, the frequency spectrum of the signal applied to the input of the analyzer is shifted to the odd harmonics of the carrier frequency. This imposes a condition on the lower limit of the carrier frequency  $\nu_c$ , in that the frequency spectrum at the higher harmonics of  $\nu_c$  must be above the central frequency  $\nu_0$  of the narrow band filter for a proper operation of the analyzer. This condition can be formulated as (see fig. 1b)

$$3 \nu_c - \nu_{c0} \geq \nu_0$$

or

$$\nu_c \geq \nu_c^{\min} = \frac{\nu_0 + \nu_{c0}}{3}$$

For  $\nu_{co} = 2 \nu_o$  we have  $\nu_c^{min} = \nu_o$ . This means that a spectrum extending up to  $\nu_{co} = 2 \nu_o$  can be still fully analyzed. (Spectra with  $\nu_{co} > 2 \nu_o$ , i.e.  $\nu_c^{min} > \nu_o$ , can be analyzed only in the restricted range  $|\nu_o - \nu_c^{min}| < \nu < \nu_{co}$  (see fig. 1 b).) The proper operation of the analyzer for input signals at frequencies above  $\nu_o$  is assured by the high input isolation of the mixers.

The response of the analyzer ("Re C" - output signal as a function of the amplitude of the input signal (300 KHz sine wave applied simultaneously to both channels) is shown in fig. 4 in a log - log representation. The slope of the straight line is two. The numbers in fig. 1a give the voltage (in mV) at the different stages of the instrument for different input signals. The channels have been made symmetrical. From the numbers in fig. 1a we infer that the response (fig. 4) is linear even for input voltages at the multipliers of 70 mV. Thus the instrument works properly for input signals (at the input of the low-pass filter) up to 350 mV.

Fig. 5 shows the "Re C" - frequency power spectrum obtained by applying a square wave (150 KHz, 100 mV) signal to both channels. The agreement with theory\* is satisfactory.

---

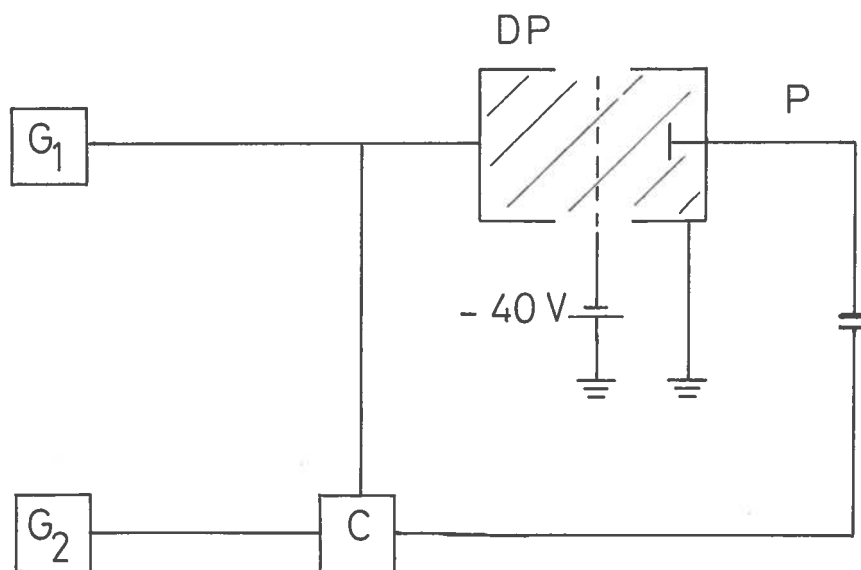

$$* \left\langle v(t)^2 \right\rangle_t \sim \left\langle \sin \omega_o t + \frac{1}{3} \sin 3 \omega_o t + \frac{1}{5} \sin 5 \omega_o t + \dots \right\rangle_t^2$$

### III. EXPERIMENTS

As a first experiment we tried to measure the cross power density spectrum for externally excited ion acoustic waves in a magnetized plasma. The waves were launched from a coarse thin wire grid and the signals derived from two other Langmuir probes were fed into the analyzer. However, the experiment failed, because the capacitively coupled pick-up signal exceeded by far the signal of the propagating ion acoustic wave, so that the Re C - output signal always measured the frequency power spectrum of the externally applied signal, independent of the distance between the two Langmuir probes. We have repeated this experiment in a DP - device, where the pick-up signal is negligible owing to a different mechanism of wave excitation. Another experiment, namely a measurement of the cross-power density spectrum of the current driven ion acoustic turbulence, has been performed with a magnetized plasma. The experimental results are reported in the following sections.

#### 1. DP - device

The experimental set-up is shown below



DP - Double Plasma Device

P - Movable Probe

C - Cross Power Spectrum Analyzer



The plasma is devided by a negatively biased fine meshed grid and a sine wave signal of frequency  $\nu$  derived from the generator  $G_1$  is applied to the housing on one side. The frequency  $\nu$  is swept over the range from 100 KHz to 800 KHz in a time  $\mathcal{T}$  ( $.1 \text{ ms} < \mathcal{T} < 1 \text{ ms}$ ); and the cross power density spectrum of the generator signal and of the signal detected by a movable probe (electron saturation current) is measured, sweeping the carrier frequency  $\nu_c$  (generator  $G_2$ ) over the range from 4 MHz to 8 MHz in a time  $t_s$  of about 1 min.. Since  $t_s$  is large compared to  $\mathcal{T}$ , the analyzer sees a white spectrum. However, only a single sine wave is excited in the plasma at a given moment. The wave propagation is one-dimensional owing to the mechanism of excitation. Figs 6 a,c,d show the frequency power spectra ( $\text{Re } C_{(0,\omega)}$ ) obtained for different conditions:

- (a,c) applying the signal of generator  $G_1$  simultaneously to both inputs with and without the DP (and plasma) in parallel. The spectrum decays with increasing frequency in case (c), since the DP represents a capacitive load.
- (d) applying the probe signal simultaneously to both inputs. The probe was about 3 cm away from the grid. The central peaks result from internal plasma noise. This noise decreases rapidly as the probe is moved away from the grid.

The results of a measurement of the real and imaginary parts of the cross power density spectrum are shown in fig.7. (The numbers give the position of the probe in millimeters.) The measured cross power density spectrum is an oscillating function as expected from equs. (7,8) for a one-directional propagation (or for a correlation of signals from single face probes), i.e. the amplitudes of  $\text{Re } C$  and  $\text{Im } C$ , are both equal to the frequency power spectrum. The dispersion relation can be derived from the period ( $\Delta\nu$ ) of the frequency oscillations. From equs. (7,8) we obtain the relation

(9) 
$$\frac{dk}{d\omega} \Delta\nu \chi = 1$$

Thus, the dispersion relation  $k(\omega)$  can be determined up to an additive constant  $k_0$  by plotting the reciprocal value of the oscillation period ( $\Delta\nu$ ) (measured for a given  $\chi$ ) versus the frequency  $\nu$  and performing the integration.

For the evaluation of our experimental results we can assume  $d\omega/dk = \omega/k = c$ . Writing equ. (9) for two different positions  $x = x_0$  and  $x = x_1 = x_0 + \Delta x$  and solving the equations for  $c$ , we obtain

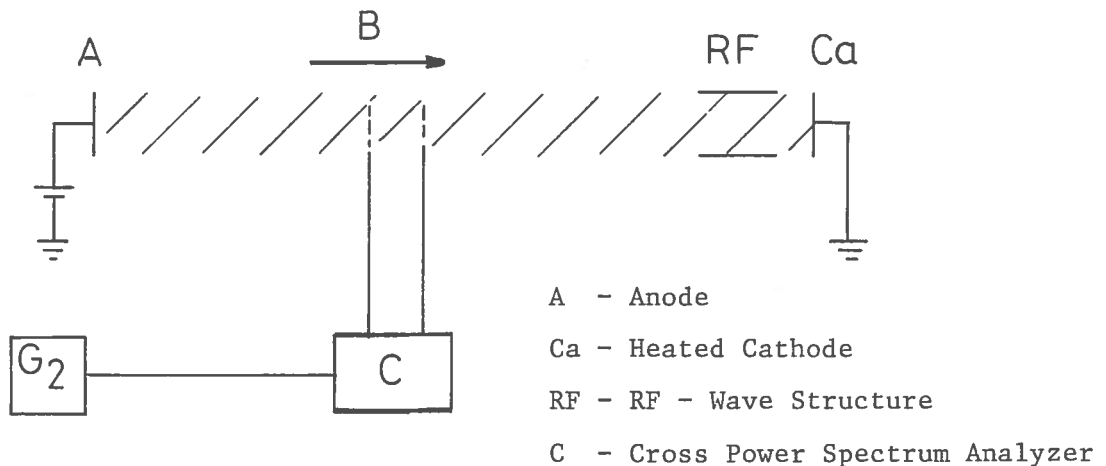
$$(10) \quad c = \frac{\Delta x}{1/\Delta\nu_1 - 1/\Delta\nu_0}$$

From the measurements in fig. 6 we find  $c \approx 2 \times 10^5$  cm/s. This value agrees well with the result of wave measurements carried out on the DP - device by means of a phase-lock technique.

The determination of the real part of the dispersion relation from a measurement of the cross power density spectrum, offers the experimental advantage that the full dispersion relation can be derived from a single measurement and that the resolution (number of experimental points) can be adjusted by an appropriate choice of the probe position (see equ. (9)).

## 2. RF - discharge

The second experiment has been performed using the arrangement shown below



The plasma is produced by resonant absorption of rf power at the electron cyclotron frequency ( $\nu_{ce} = 1.1$  GHz) and an electron current is drawn along the plasma column by applying a dc voltage between a hot electron emitting cathode and a disk anode. An ion acoustic instability is excited, if the electron drift velocity exceeds the ion sound speed /3/. Figs. 8 a-c show the results of a measurement of the real and imaginary parts of the cross power density spectrum. The measurements have been performed by means of two movable grid probes, which have been kept on dc floating potential, to minimize the disturbance of the plasma.

The experimental results allow the following conclusions:

1. Re C and Im C are oscillating functions, i.e. the excited noise follows a dispersion relation. As the oscillation period  $\Delta\nu$  is constant over the frequency range of the instability, we may assume that the dispersion relation is linear ( $k = \frac{\omega}{c}$ ). The experimental value for  $c = \Delta\nu\lambda = 2.3 \times 10^5$  cm/s agrees with the value of the ion sound velocity, which has been previously found from the propagation of ion acoustic test waves.
2. The amplitude of the oscillating functions Re C and Im C is equal and agrees well with the frequency power spectrum. From a consideration of equs (7,8)\*, -and taking into account that the measurements have been performed with grid probes, which look simultaneously in both directions of the plasma column,- we conclude that the excited ion acoustic waves all propagate in one direction. This is in agreement with the theoretical prediction that only waves, which propagate in the direction of the current, are destabilized.

---

\* Equs. (7,8) can only be applied, if the ion acoustic turbulence can be considered as one-dimensional. This is the case, as the instability occurs at frequencies well above the ion cyclotron frequency /4/.

We gratefully acknowledge the valuable discussions with  
Mr. J.-P. Perotti.

REFERENCES

- /1/ J. Max, "Méthodes et Techniques de TRAITEMENT DU SIGNAL et Application aux Mesures Physiques, Masson et Cie (1972)
- /2/ K.J. Harker and D.B. Ilić, Rev. Sci. Instrum. 45, 1315 (1974)
- /3/ M. Bitter and P.J. Paris, LRP 119/76
- /4/ A. Hirose, I. Alexeff and W.D. Jones, Phys. Fluids 1290 and 1414, 13 (1970)

Figure Captions

Figure 1: (a) Block-diagram of the analyzer.  $A_1$ ,  $A_2$  - (Motorola 733) amplifier ;  $F_1$  - Krohn - Hile 3103 Filter, (passband variable in the range from 10 Hz to 3 MHz); narrow band ( $6 \pm .018$  MHz) quartz filter ;  $M_1$  - (HP 10534 A) Mixer ; PS - 90 degree phase shifter ;  $M_u$  - (Motorola MC 1496) Multiplier ;  $A_3$  - (Motorola 741) amplifier. The number give the voltage at the different stages of the instrument in millivolts. The input signals have been applied to the input of the low pass filter  $F_1$  for these measurements. The gain of the amplifier  $A_1$  is variable between 8 and 100.

(b) Principle of operation: The spectrum of the input signal, which extends to  $\nu = \nu_{co}$ , is shifted up in frequency by the mixer and swept over the window of the narrow band-pass filter  $F_2$  at  $\nu_o = 6$  MHz by varying the carrier frequency  $\nu_c$ . Thus, the multiplication of the "in phase" signals and of the "90 degree out of phase" signals is performed at a single frequency  $\nu_o$ . The time averages of the products are proportional to the real and imaginary parts of the cross power density spectrum.

(c) Detailed circuit. The 90 degree phase shift is performed by a cable of an appropriate length.

Figure 2: Frequency response of the quartz filters. The oscillogram has been taken applying a sine wave of 10 mV amplitude to the filters and sweeping the frequency over the range from 5.965 MHz to 6.035 MHz. The vertical scale is 5 mV/cm

- Figure 3: Output signal of the mixer obtained for a carrier signal (sine wave, 5.5 MHz) of 1.5 volt amplitude and a modulating signal (sine wave, 500 KHz) of  $40 \text{ mV}_{pp}$ . (vertical scale: 20 mV/cm, horizontal scale: . 5  $\mu\text{s}/\text{cm}$  and . 2  $\mu\text{s}/\text{cm}$ , respectively).
- Figure 4: "Re C" - output signal as a function of the amplitude of the signal applied to the inputs of the filters  $F_1$ .
- Figure 5: "Re C" - frequency power spectrum obtained by applying a square wave signal of 150 KHz to both channel inputs.
- Figure 6:
- (a,c) "Re C" - frequency power spectrum obtained by applying sine wave signal to both inputs (c) with and (a) without the DP (and plasma) in parallel. The frequency is swept from 100 KHz to 800 KHz.
  - (b) "Im C" - output signal obtained for the same conditions.
  - (d) "Re C" - frequency spectrum measured by a probe at a distance of 3 cm away from the grid.
- Figure 7: Real and imaginary part of the cross power density spectrum. The numbers give the position of the probe in millimeters.
- Figure 8: Frequency power spectrum, and real and imaginary part of the cross power density spectrum obtained for an electron current of 180 mA. The distance of the two Langmuir probes was 2.5 cm.

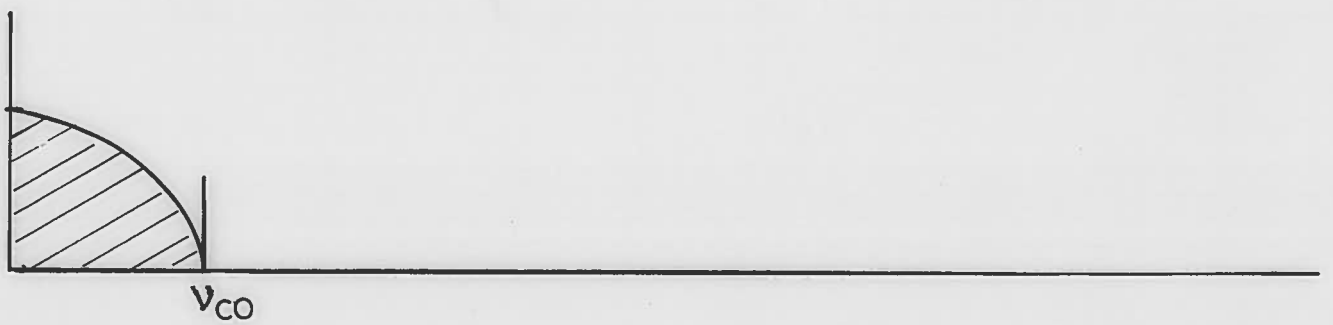
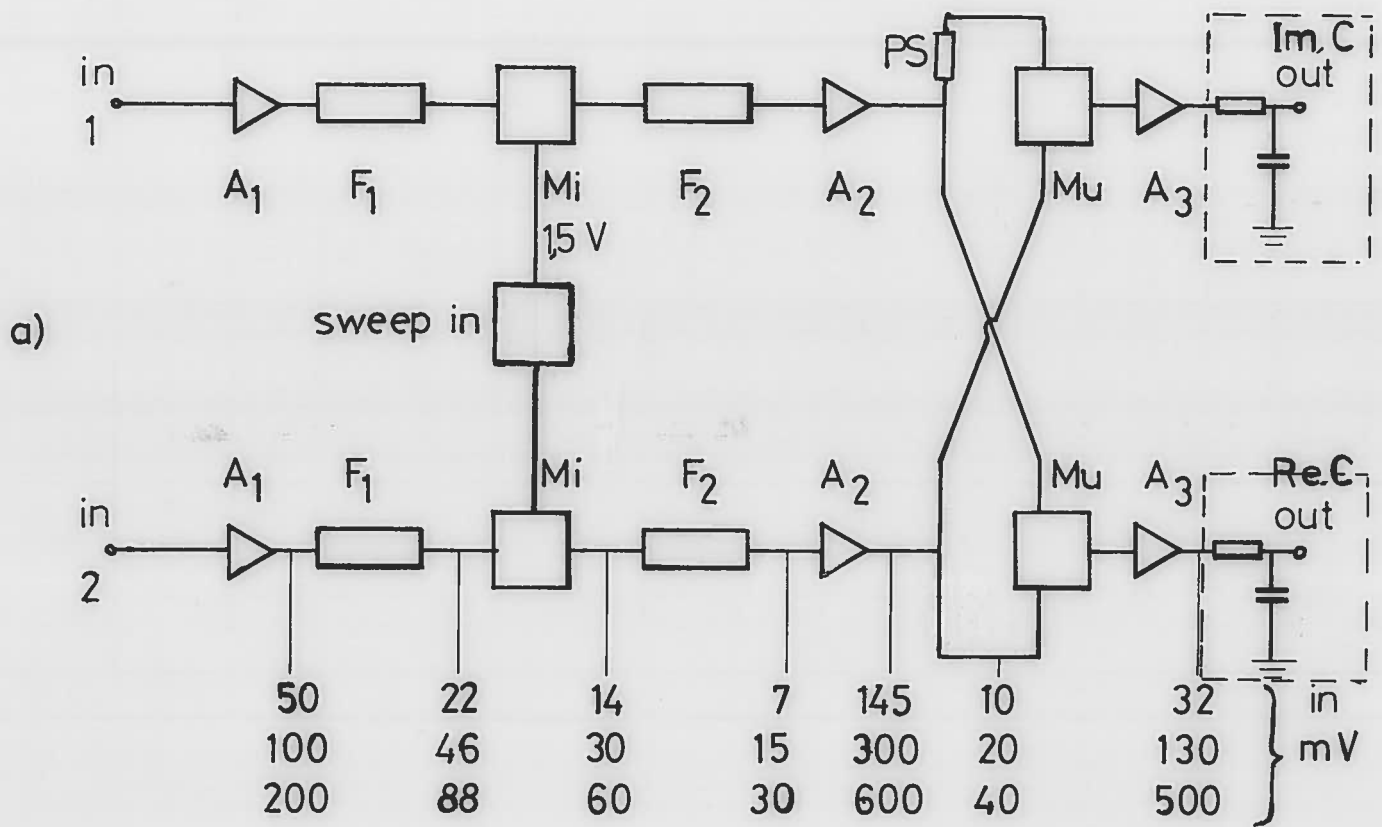
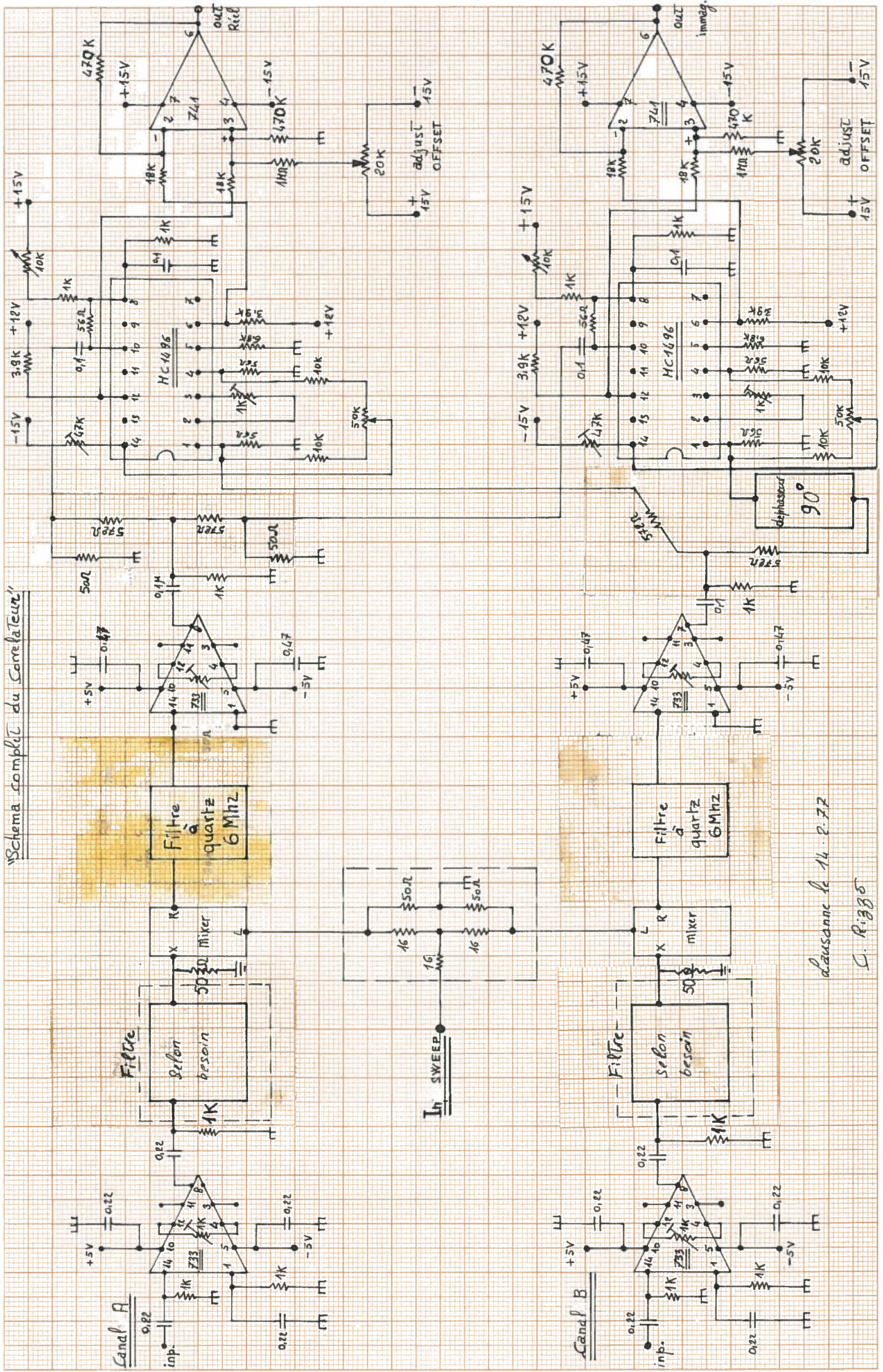


Fig.1



Schema complet du Corrélateur



lausanne le 14.2.77  
C. Riggs

Fig. 1c)

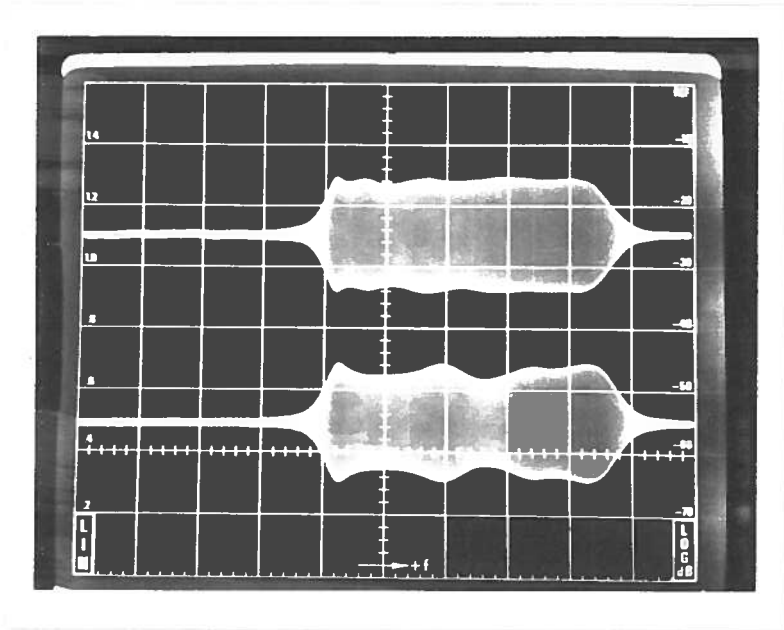


Fig. 2

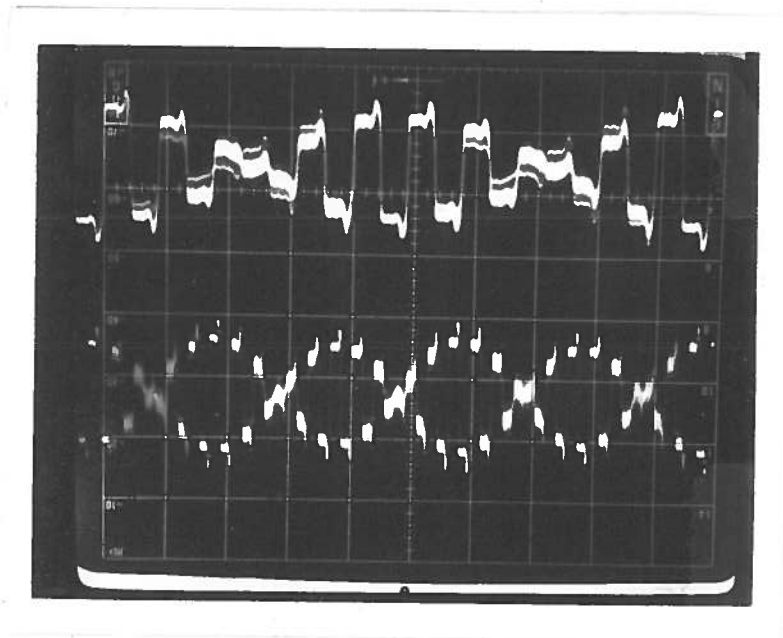
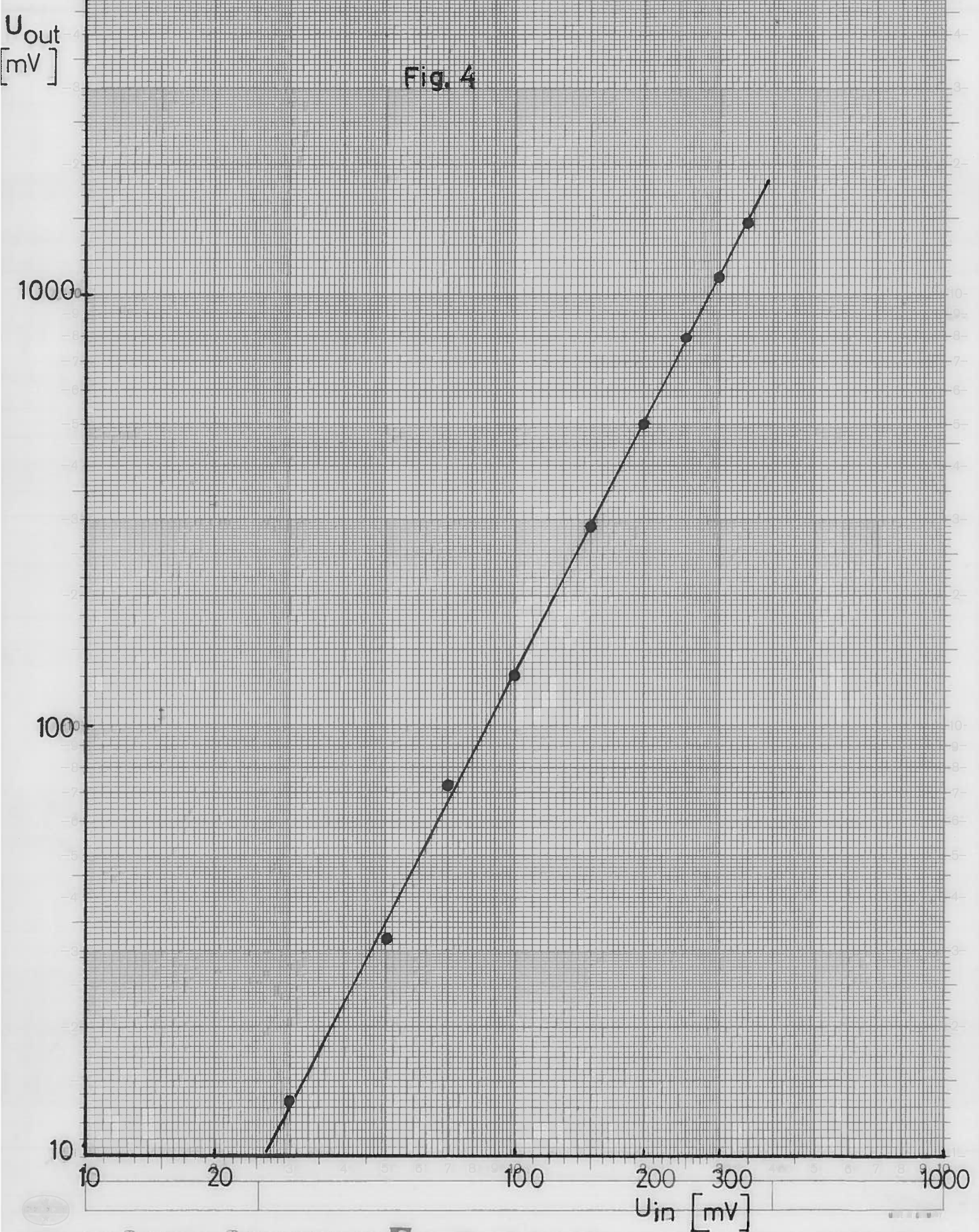


Fig. 3

Fig. 4



$\nu_0 = 150 \text{ KHz}$

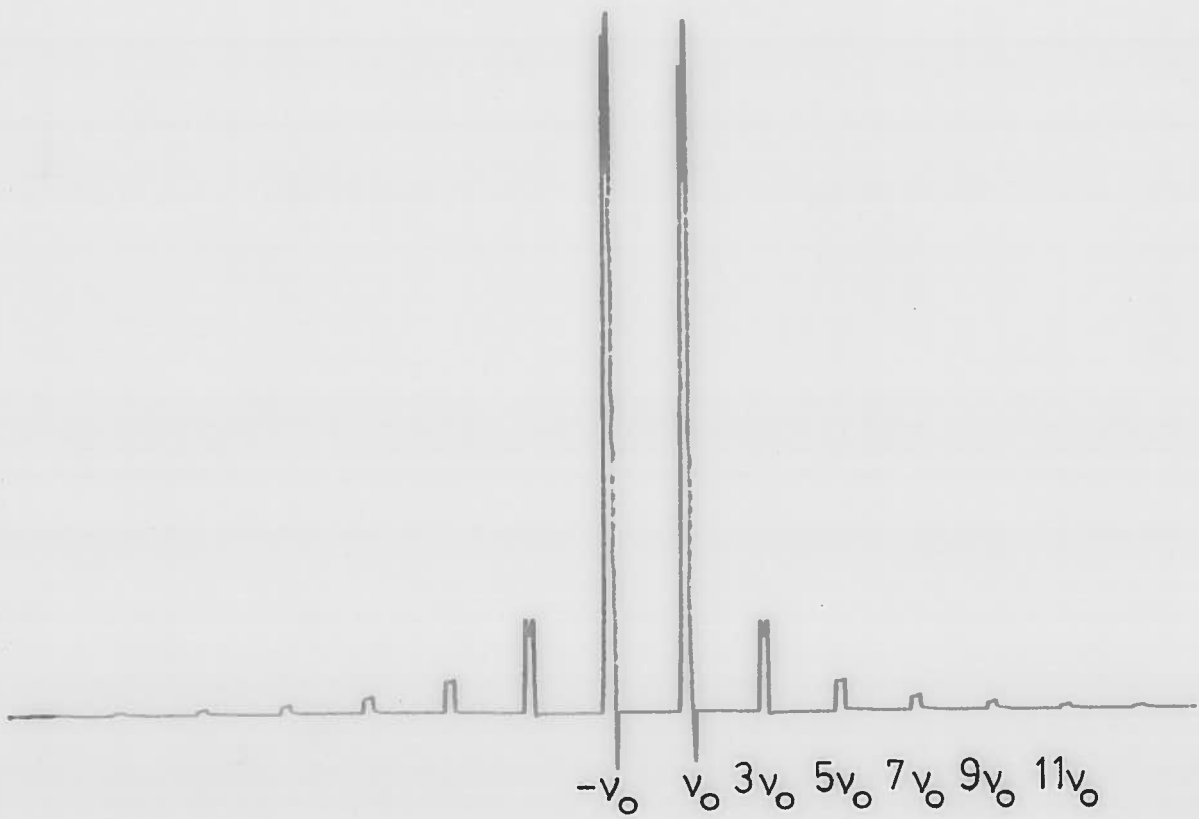


Fig. 5

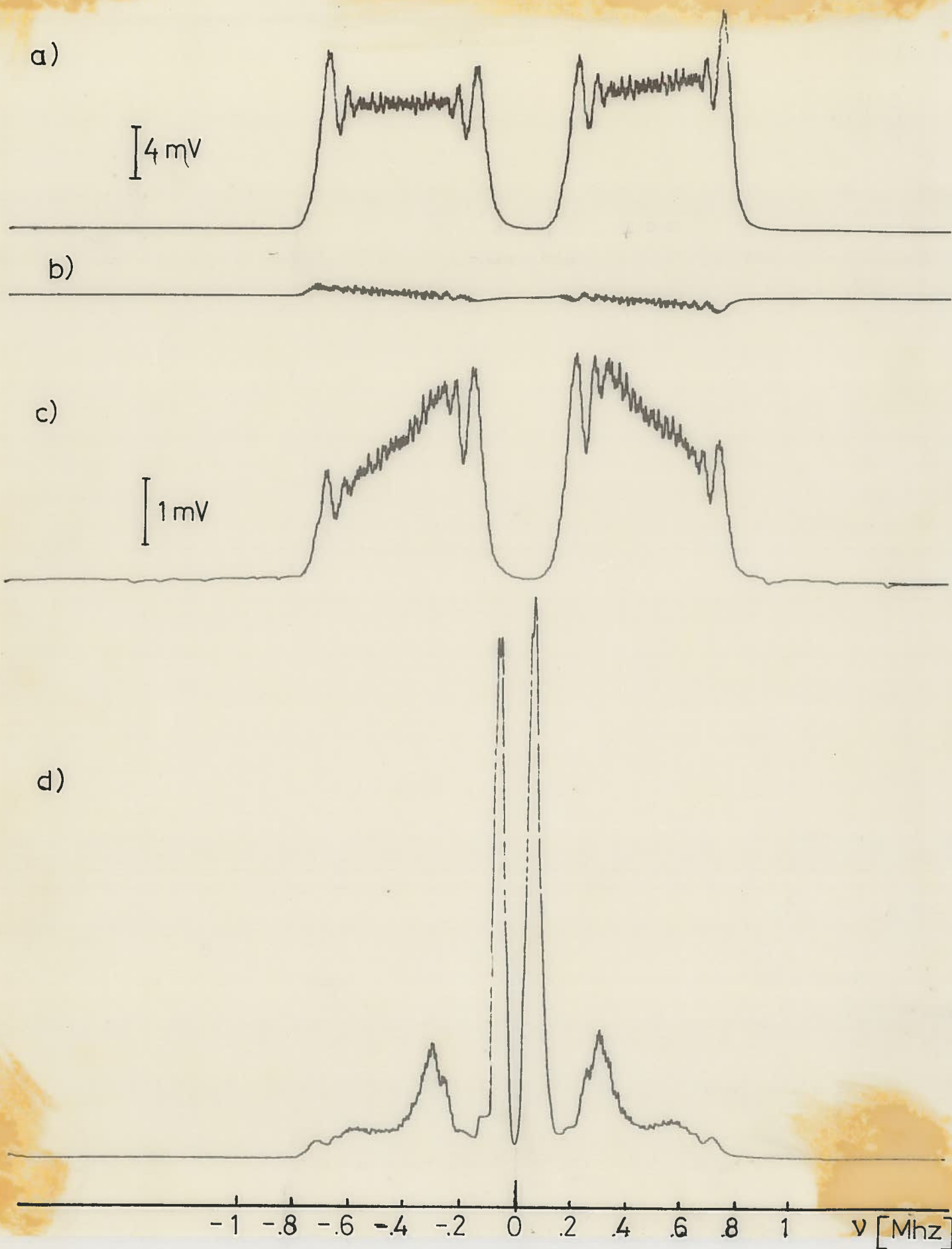
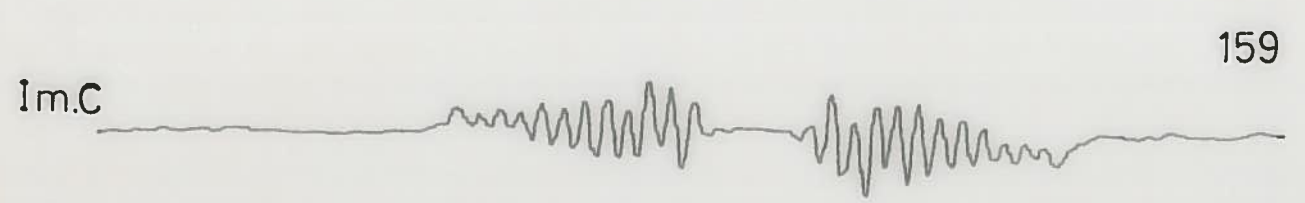
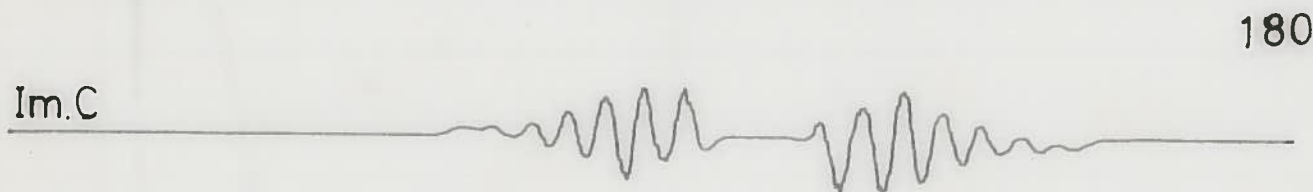
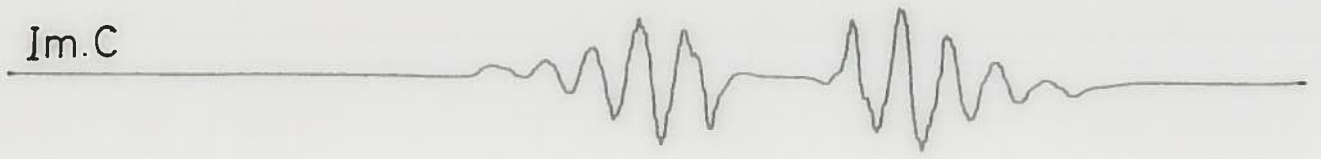
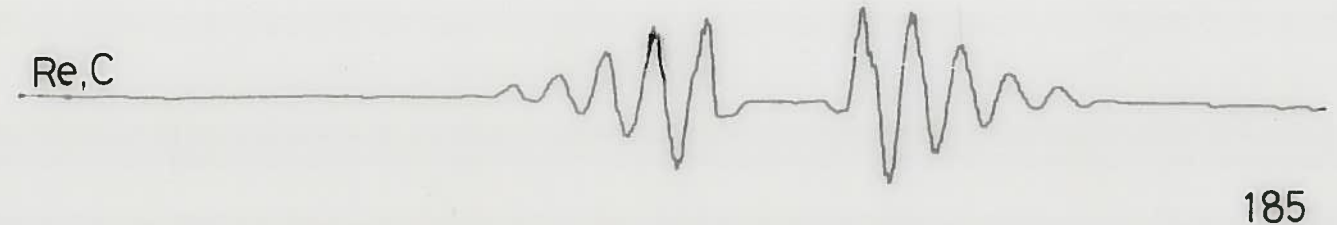


Fig. 6



Driver: 200 mV

Fig. 7



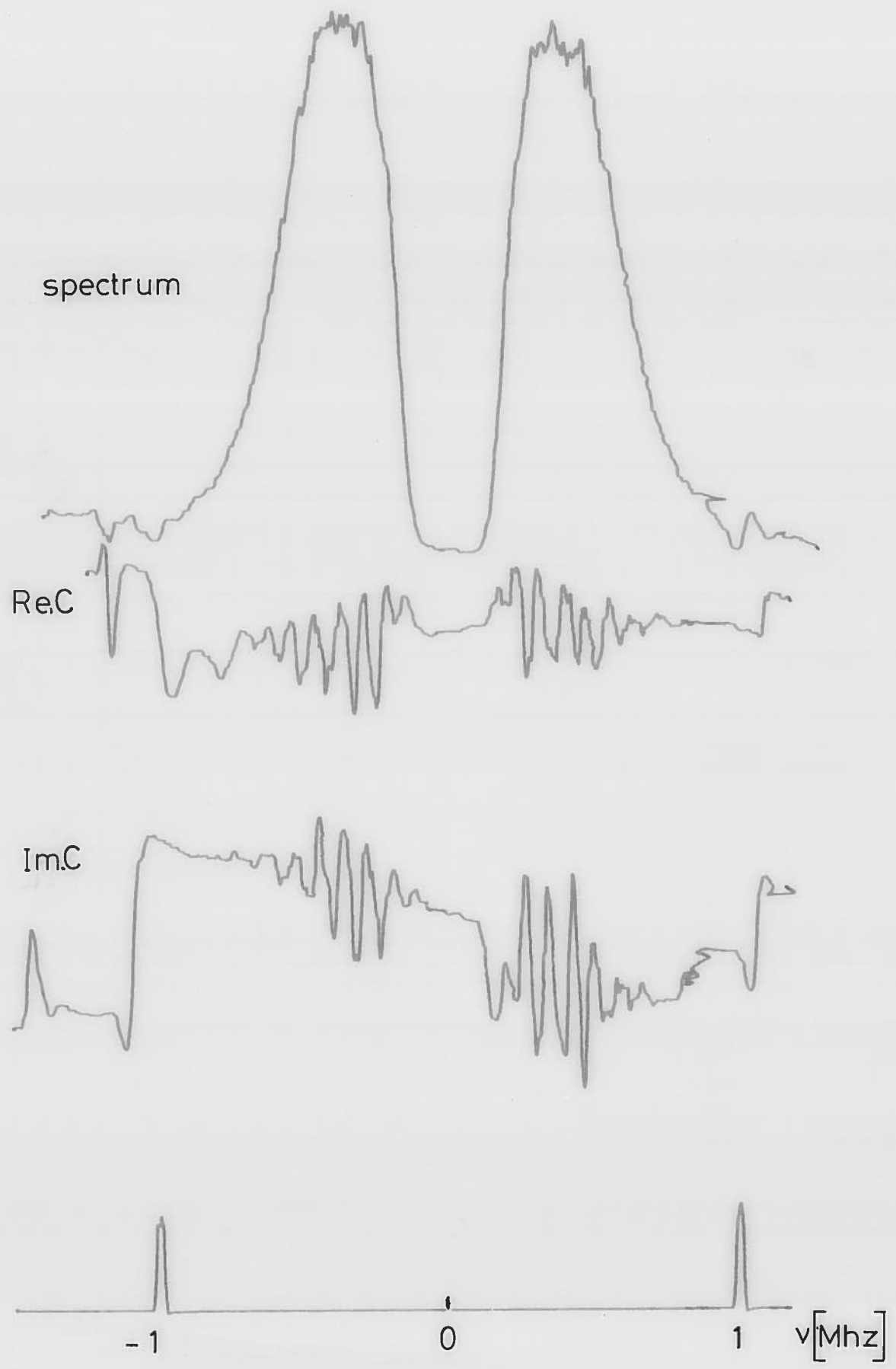


Fig.8